PLOS ONE

RESEARCH ARTICLE

Identification of hub genes associated with COVID-19 and idiopathic pulmonary fibrosis by integrated bioinformatics analysis

Qianyi Chen[1], Shilin Xia[2,3]*, Hua Sui[1], Xueying Shi[1,2], Bingqian Huang[1,2], Tingxin Wang[1]

1 Institute (College) of Integrative Medicine, Dalian Medical University, Dalian, Liaoning, China, **2** Clinical Laboratory of Integrative Medicine, The First Affiliated Hospital of Dalian Medical University, Dalian, Liaoning, China, **3** Department of Palliative Medicine, Graduate School of Medicine, Juntendo University, Tokyo, Japan

* xiashilin@dmu.edu.cn

OPEN ACCESS

Citation: Chen Q, Xia S, Sui H, Shi X, Huang B, Wang T (2022) Identification of hub genes associated with COVID-19 and idiopathic pulmonary fibrosis by integrated bioinformatics analysis. PLoS ONE 17(1): e0262737. https://doi.org/10.1371/journal.pone.0262737

Editor: Chandrabose Selvaraj, Alagappa University, INDIA

Received: October 7, 2021

Accepted: January 4, 2022

Published: January 19, 2022

Peer Review History: PLOS recognizes the benefits of transparency in the peer review process; therefore, we enable the publication of all of the content of peer review and author responses alongside final, published articles. The editorial history of this article is available here: https://doi.org/10.1371/journal.pone.0262737

Data Availability Statement: All data generated or analyzed during this study are included in this published article and its supplementary information files.

Abstract

Introduction

The coronavirus disease 2019 (COVID-19), emerged in late 2019, was caused by severe acute respiratory syndrome coronavirus 2 (SARS-CoV-2). The risk factors for idiopathic pulmonary fibrosis (IPF) and COVID-19 are reported to be common. This study aimed to determine the potential role of differentially expressed genes (DEGs) common in IPF and COVID-19.

Materials and methods

Based on GEO database, we obtained DEGs from one SARS-CoV-2 dataset and five IPF datasets. A series of enrichment analysis were performed to identify the function of upregulated and downregulated DEGs, respectively. Two plugins in Cytoscape, Cytohubba and MCODE, were utilized to identify hub genes after a protein-protein interaction (PPI) network. Finally, candidate drugs were predicted to target the upregulated DEGs.

Results

A total of 188 DEGs were found between COVID-19 and IPF, out of which 117 were upregulated and 71 were downregulated. The upregulated DEGs were involved in cytokine function, while downregulated DEGs were associated with extracellular matrix disassembly. Twenty-two hub genes were upregulated in COVID-19 and IPF, for which 155 candidate drugs were predicted (adj.P.value < 0.01).

Conclusion

Identifying the hub genes aberrantly regulated in both COVID-19 and IPF may enable development of molecules, encoded by those genes, as therapeutic targets for preventing IPF progression and SARS-CoV-2 infections.

Funding: The author(s) received no specific funding for this work.

Competing interests: The authors have declared that no competing interests exist.

Introduction

Severe acute respiratory syndrome coronavirus 2 (SARS-CoV-2), a novel enveloped RNA beta coronavirus, is accountable for an ongoing outbreak of coronavirus disease 2019 (COVID-19) [1,2], which constitutes an enormous global burden on society. COVID-19 has resulted in over 224 million confirmed cases and over 4.68 million deaths globally. The research and development of anti-COVID-19 vaccine is currently ongoing; moreover, controlling disease transmission requires the development of effective drugs to cure it.

Idiopathic pulmonary fibrosis (IPF) is a chronic progressive disease with an irreversible advanced lung failure. IPF patients suffer from lung function decline, respiratory failure, and ultimately death [3]. The risk factors for IPF and COVID-19 are reported to be common [4]. However, the molecular mechanism underlying a crosstalk between COVID-19 and IPF was poorly defined. Identification of novel molecular targets has thus become imperative for the advancement of targeted therapy for COVID-19 with antifibrotic strategies.

The goal of the current study was to investigate the potential role of differentially expressed genes (DEGs) in the association between COVID-19 and IPF. We performed an overlap of DEGs between two the diseases on a basis of 5 datasets, followed by distinguishing the upregulated and downregulated genes. Based on a series of enrichment analysis, we interpreted the function of upregulated and downregulated DEGs. Furthermore, we carried out a protein-protein interaction (PPI) network analysis in which 22 upregulated hub genes and 11 downregulated hub genes were identified. Then, we analyzed the prominent function of 22 hub genes, and it was revealed that these hub genes upregulated in COVID-19 and IPF were involved in cytokine mediation, such as cell response to interferon. Finally, we performed a drug-target analysis and 155 candidate drugs targeting upregulated hub genes were identified. The workflow of the current study is shown in Fig 1. Herein, our findings demonstrated that hub gene and the candidate drug will be beneficial to the COVID-19 treatment. We also provide an insight that we can design and develop a candidate drug against virus variant such as Delta SARS-CoV-2, when there are common risk factors between a different disease and that caused by Delta.

The high-throughput data of SARS-CoV-2 infection was obtained from biopsy of a COVID-19 patient in GSE147507. The data of IPF was obtained from biopsy of IPF patient in five datasets, including GSE13065, GSE110147, GSE1i01286, GSE53845, and GSE24206. Venn diagram was used to reveal overlapped DEGs. The magenta circle represents DEGs in GSE147507 and yellow one represents DEGs in IPF datasets. Subsequently, common DEGs were subjected to a series of enrichment analysis and PPI network investigation. Based on an identification of highly expressed hub genes, a candidate drug was predicted to be available for a crosstalk between COVID-19 and IPF during the COVID-19 therapy.

Materials and methods

The collection of databases and the identification of DEGs

DEGs were obtained from six datasets in Gene Expression Omnibus (GEO, https://www.ncbi.nlm.nih.gov/geo/) database [5,6] The DEGs related to SARS-CoV-2 were obtained from GSE147507 including SARS-CoV-2 infection in lung epithelium and lung alveolar cells of humans in Apr 07, 2021 [7,8]. Five GEO datasets were collected to obtain the DEGs related to IPF, including GSE13065 with 3 IPF samples and 3 normal samples lastly updated in May 02, 2019 [9], GSE110147 with 22 IPF samples and 11 normal samples lastly updated in Aug 19, 2018 [10], GSE101286 with 12 IPF samples and 3 normal samples lastly updated in Jul 25, 2021 [11], GSE53845 with 40 IPF samples and 8 normal samples lastly updated in Jan 23, 2019 [12],

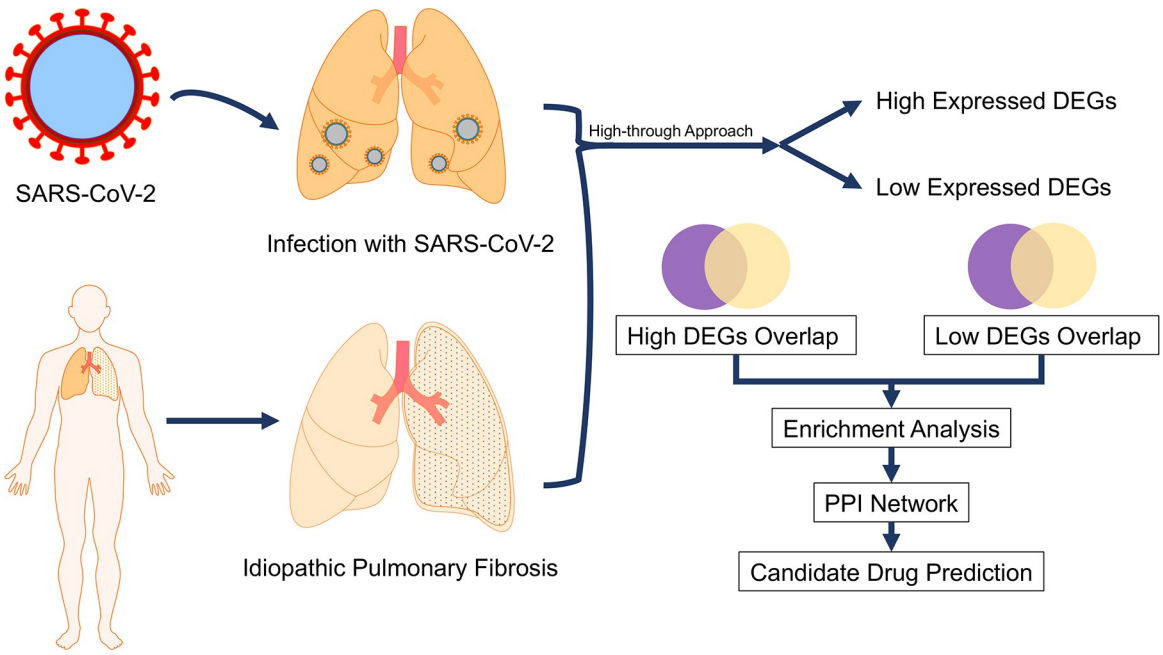

Fig 1. The workflow of the current study.

https://doi.org/10.1371/journal.pone.0262737.g001

and GSE24206 with 17 IPF samples and 6 normal samples lastly updated in Mar 25, 2019 [13]. DEGs for the datasets were analyzed through GEO2R (https://www.ncbi.nlm.nih.gov/geo/geo2r/) web tool which uses limma package for identifying DEGs and visualized by ggplot 2 in R package. Benjamini-Hochberg method was applied to both the datasets for controlling of false discovery rate (FDR). Cut-off criteria was obtained for GSE147507 using adjusted P-value < 0.05 and log2-fold change (absolute) > 1.0. All data generated or analyzed during this study are included in this published article and its supplementary information files.

Identification of common genes between COVID-19 and IPF

To determine detailed information of DEGs, these genes were further divided by aberrant expression level in distinct database. The adjusted P-value < 0.05 and log2-fold change > 1.0 is used as cut-off criteria for high expression DEGs, and adjusted P-value < 0.05 and log2-fold change < -1.0 for low expression DEGs in distinct dataset.

The upregulated as well as downregulated DEGs in GSE147507 were overlapped with other five datasets related to IPF.

Enrichment analysis for common DEGs

To understand a functional characteristic of DEGs in COVID-19 and IPF, a series of enrichment analysis were adopted to gain a detailed information of biological function and pathways. Gene Ontology (GO) was performed to provide three terms, including biological process, molecular function, and cellular component [14]. Kyoto Encyclopedia of Genes and Genomes (KEGG) was used to identify metabolic pathway [15]. An online tool Enrichr (https://amp.pharm.mssm.edu/Enrichr/) was carried out to enrich the significant pathways, including WikiPathways, Reactome, and BioCarta database [16,17]. Based on the enrichment analysis, we concentrated on biological function of DEGs in both COVID-19 and IPF.

PPI network analysis for the identification of hub genes

For assessing an association between DEGs, we established a PPI network on the Search Tool for the Retrieval of Interacting Genes (STRING) (https://string-db.org/) [18], which was utilized to predict physical and functional associations between proteins. Subsequently, we determined hub genes via an analysis of Cytohubba and MCODE on Cytoscape (3.8.2). Cytohubba (http://apps.cytoscape.org/apps/cytohubba) is a plugin of Cytoscape to explore protein associations according to topological algorithms. Top 10 hubba node was set to obtain the hub genes from DEGs. Molecular Complex Detection (MCODE) (http://apps.cytoscape.org/apps/mcode) is another plugin to provide clusters of subnetworks. The parameter of MCODE is Degree Cutoff = 2, Node score cutoff = 2, and K-score = 2.

Prediction of candidate drugs for hub genes

The final stage of the study was designed to determine candidate drug for highly expressed hub genes. The access of the Drug Signatures database (DSigDB) is acquired through Enrichr (https://amp.pharm.mssm.edu/Enrichr/) platform, which contains the largest number of drugs/compound-related gene sets to date, were extracted and compiled from quantitative inhibition data of drugs/compounds from a variety of databases and publications [19]. Enrichr is mostly used as an enrichment analysis platform that represents numerous visualization details on collective functions for the genes that are provided as input. We predicted candidate drug targeted hub gene. The adj.P.value < 0.01 was considered statistically significant. The candidate drugs can be sorted by adj.P.value and combined score ranking.

Results

Identification of common DEGs between COVID-19 and IPF

From GSE147507 dataset, we identified 812 DEGs including 396 upregulated genes and 417 downregulated genes (Fig 2). Out of 5977 DEGs identified from five IPF GEO datasets, 2369 were upregulated and 3608 were downregulated. We then overlapped DEGs from one SARS-CoV-2-infected sample dataset and five IPF datasets. A total of 117 and 71 genes were identified as common upregulated (Fig 3A) and downregulated DEGs (Fig 3B), respectively. Next, we tried to identify the function of common DEGs involved during the progression of COVID-19 and IPF.

GO and pathway identification by gene set enrichment analysis

To further understand the function and pathways of common DEGs, enrichment analysis was preformed to show that common upregulated DEGs in COVID-19 and IPF were involved in cytokine mediation, such as cell response to interferon (Fig 4, Table 1). The DEGs downregulated in both the diseases, however, were associated in the disassembly of cellular components and extracellular matrix (Fig 5, Table 2). The upregulated DEGs were mainly located in cellular component, and main molecular function of these genes was found to bind to small molecules and metabolites. Among upregulated DEGs, 25 genes were involved in cytokine-mediated signaling pathway and 11 genes were involved in cellular response to type I interferon and 11 genes in type I interferon signaling pathway in GO terms. The downregulated DEGs located at the intracellular membrane organelle and nucleus, appeared to bind with RNA and catalytic enzymes, and mediate channel activity. The GO results were consistent with those of a serial pathway analysis, including KEGG, Reactome, wikipathway, and Biocarta. For instance, Reactome and wikipathway revealed that upregulated DEGs were related to interferon signaling

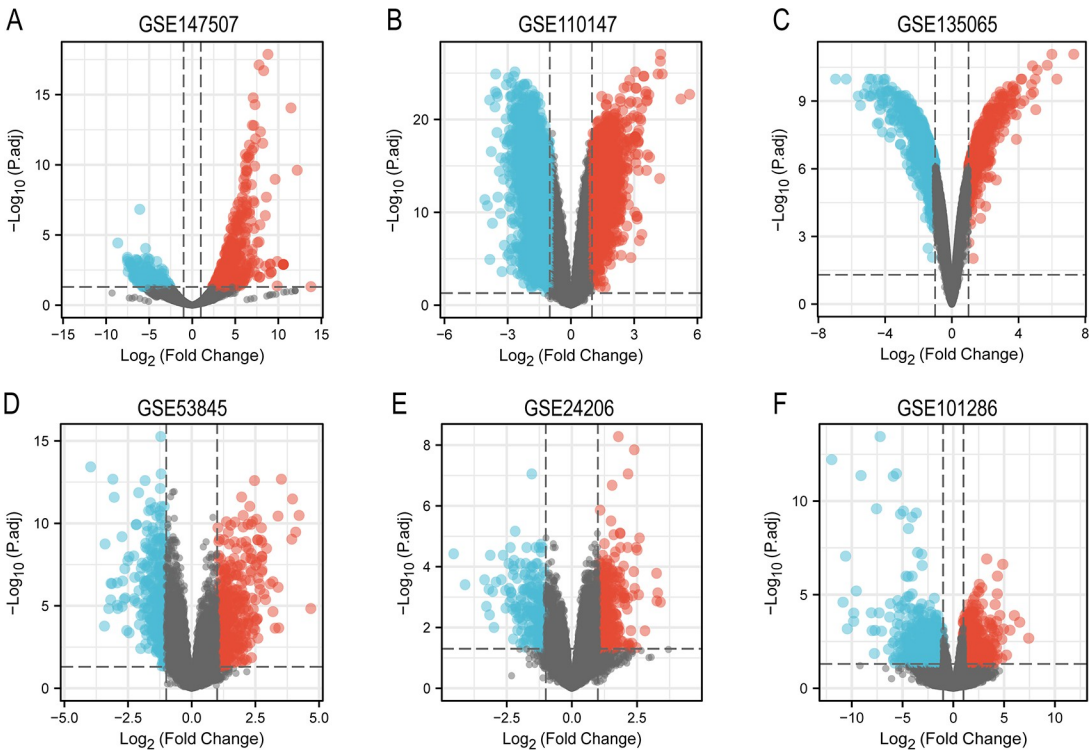

Fig 2. Volcano plot of differentially expressed gene from COVID-19 patient samples and IPF patient samples. A: Volcano plot of differentially expressed genes between uninfected human lung biopsies and that of deceased COVID-19 patient. B-F: Volcano plot of differentially expressed genes between lung samples from IPF patients and healthy control. The red plots with $|\log FC| > 1$ and P value < 0.05 represent upregulated genes and blue represents downregulated genes.

https://doi.org/10.1371/journal.pone.0262737.g002

and cytokine signaling pathway (S1 Fig), and downregulated DEGs were involved in MMP activation and collagen degradation (S2 Fig). Overall, these results indicated that upregulated and downregulated DEGs influenced entirely different biological functions.

Identification of hub genes via PPI network analysis

The PPI network analysis revealed an association of DEGs between COVID-19 and IPF. Among 117 upregulated DEGs, 22 hub genes were identified on the basis of Cytohubba and MCODE analysis, including MX1, CCL2, CXCL10, TYROBP, STAT1, S100A12, IRF7, IL1B, TREM1, SPI1, UBE2L6, IFI44L, XAF1, IRF9, EPSTI1, ISG15, OASL, IFITM1, CMPK2, IFI6, OAS2, IFITM3. Among 71 downregulated DEGs, 11 hub genes were identified, including HMOX1, PPIG, MPHOSPH10, GNL2, MMP1, GADD45A, UTP6, TSR1, CCND1, PRMT1, URB1 (Fig 6).

Enrichment analysis of hub genes

The GO enrichment analysis revealed that the 22 hub genes were upregulated in cellular response to type I interferon and type I interferon signaling pathway. The analysis also exhibited significant involvement of mitochondrial envelope and adenylyl transferase activity in the upregulated group (S3 Fig). In the downregulated group, 11 hub genes mostly enriched in nucleolus and nuclear lumen, were appeared to be evolved in RNA binding and mitotic G1 DNA damage checkpoint signaling (S4 Fig).

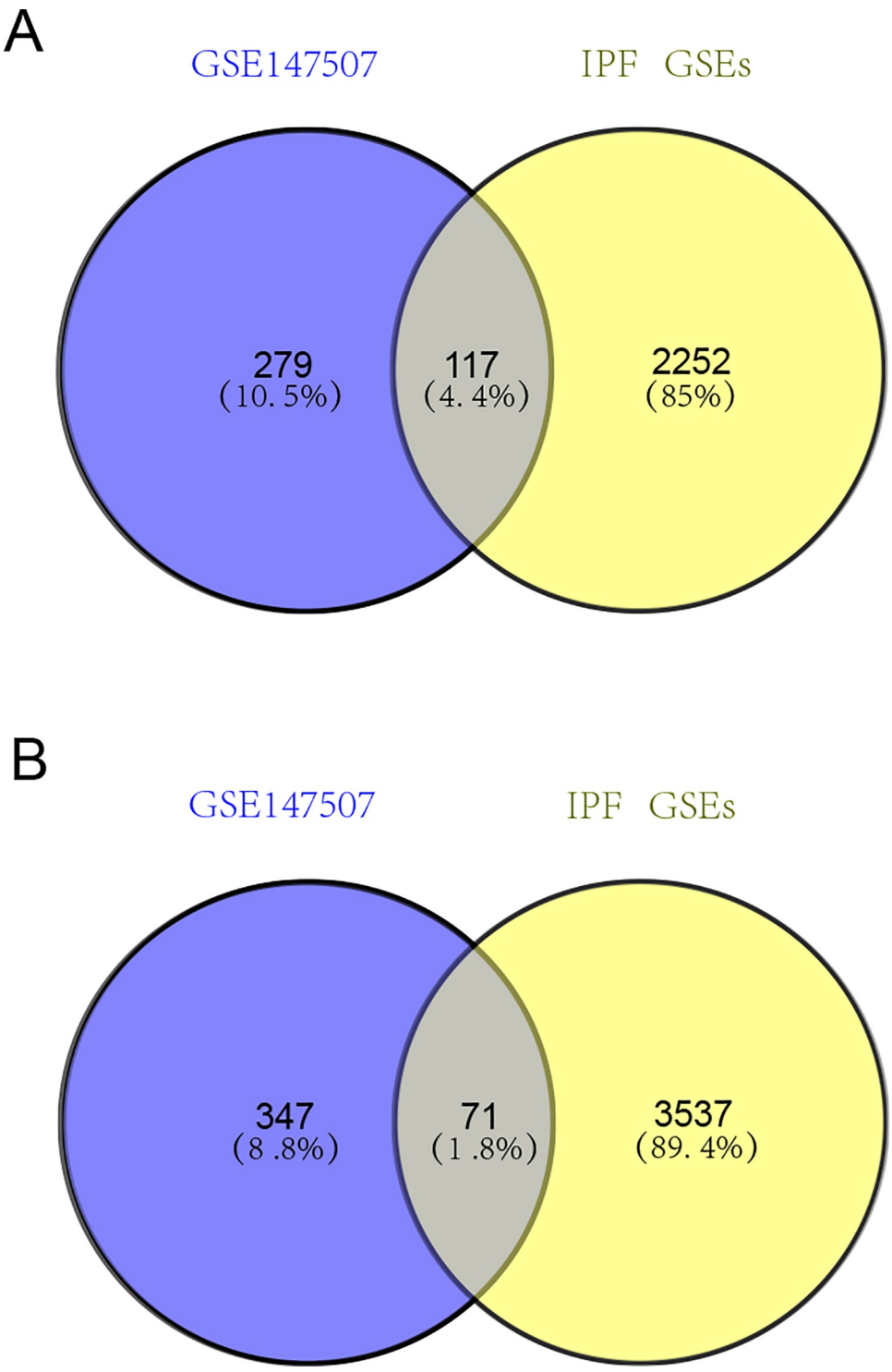

Fig 3. Venn diagram showing differentially expressed genes between COVID-19 and IPF. A: Upregulated DEGs between COVID-19 and IPF. B: Downregulated DEGs between COVID-19 and IPF. The blue circle in Venn diagram represents DEGs in COVID-19 dataset, and yellow circle represents five DEGs in IPF datasets.

https://doi.org/10.1371/journal.pone.0262737.g003

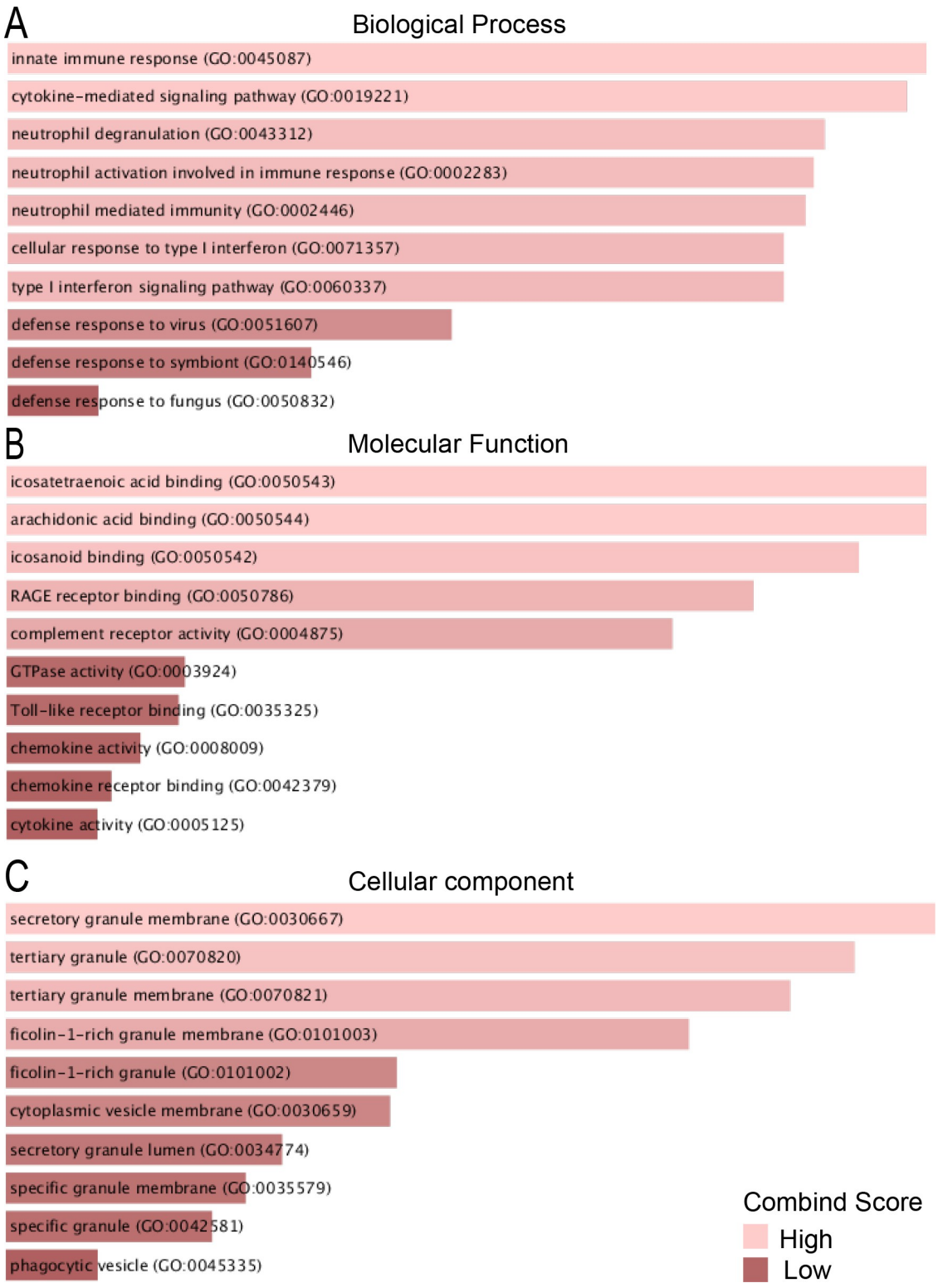

Fig 4. GO terms of upregulated DEGs between COVID-19 and IPF. A: GO analysis of upregulated DEGs related to biological process. B: GO analysis of upregulated DEGs related to molecular function. C: GO analysis of upregulated DEGs related to cellular component.

https://doi.org/10.1371/journal.pone.0262737.g004

Table 1. Go enrichment analysis of upregulated DEGs between COVID-19 and IPF.

Category	GO ID	GO Pathways	P-values	Genes
GO biological process	GO:0045087	innate immune response	9.38704192 9923436E-15	IFITM3;IFITM1;CR1;FCER1G;GCH1;MX1;IFI6; ISG15;RNASE2;TREM1;SIRPB1;CXCL16; CXCL10;CLEC4D;TYROBP;CLEC7A; IRF7;S100A12;CLEC4E
	GO:0019221	cytokine-mediated signaling pathway	1.150606954 6074619E-14	IFITM3;IFITM1;CSF3R;SPI1;FPR1; IFI6;IL27;IL2RG;OASL;CA1;CCL2; HLA-DRB5;FCER1G; STAT1;IL1R2;MX1;ISG15;CXCL10; IL1A;OAS2;IL1B;IRF7;PELI1;XAF1;IRF9
	GO:0043312	neutrophil degranulation	4.286470567 853142E-14	MGAM;CR1;FCER1G;GCA;GMFG; FPR1;GPR84;FPR2;RNASE2;MMP8;SIRPB1; PLAC8;MMP25;CLEC4D;TYROBP;SELL; S100A12;OLR1;CYSTM1;S100A9;S100A8; SIGLEC5
	GO:0002283	neutrophil activation involved in immune response	5.071176119 881218E-14	MGAM;CR1;FCER1G;GCA;GMFG;FPR1; GPR84;FPR2;RNASE2;MMP8;SIRPB1;PLAC8; MMP25;CLEC4D;TYROBP;SELL;S100A12; OLR1; CYSTM1;S100A9;S100A8;SIGLEC5
	GO:0002446	neutrophil mediated immunity	5.7466938301 88601E-14	MGAM;CR1;FCER1G;GCA;GMFG;FPR1; GPR84;FPR2;RNASE2;MMP8;SIRPB1;PLAC8; MMP25;CLEC4D;TYROBP;SELL;S100A12; OLR1;CYSTM1;S100A9;S100A8;SIGLEC5
	GO:0071357	cellular response to type I interferon	9.6100294957 7372E-14	IFITM3;IFITM1;OAS2;STAT1;MX1;IRF7;IFI6; ISG15;XAF1;IRF9;OASL
	GO:0060337	type I interferon signaling pathway	9.610029495 77372E-14	IFITM3;IFITM1;OAS2;STAT1;MX1;IRF7;IFI6; ISG15;XAF1;IRF9;OASL
	GO:0051607	defense response to virus	1.557313565 1590148E-11	IFITM3;CXCL10;IFITM1;OAS2;STAT1;MX1; IRF7;IFI6;ISG15;RNASE2;IFI44L;OASL
	GO:0140546	defense response to symbiont	1.369319174 8252762E-10	IFITM3;IFITM1;OAS2;STAT1;MX1;IRF7;IFI6; ISG15;RNASE2;IFI44L;OASL
	GO:0050832	defense response to fungus	3.9184743402 451796E-9	CLEC4D;CLEC7A;S100A12;CLEC4E;S100A9; S100A8
GO Molecular Function	GO:0030667	secretory granule membrane	6.097577975166167E-10	MGAM;CR1;FCER1G;FPR1;GPR84;FPR2; SIRPB1; MMP25;CLEC4D;TYROBP;SELL;OLR1; CYSTM1; SIGLEC5
	GO:0070820	tertiary granule	2.7444531601972747E-9	MGAM;CLEC4D;CR1;FCER1G;FPR1;OLR1; CYSTM1;GPR84;FPR2;MMP8;SIGLEC5
	GO:0070821	tertiary granule membrane	9.197680245668367E-9	MGAM;FCER1G;CLEC4D;OLR1;CYSTM1; FPR2; GPR84;SIGLEC5
	GO:0101003	ficolin-1-rich granule membrane	5.8340251207518634E-8	MGAM;CR1;FCER1G;CLEC4D;FPR1;FPR2; SIGLEC5
	GO:0101002	ficolin-1-rich granule	1.1269234942705415E-5	MGAM;CLEC4D;CR1;FCER1G;GMFG;FPR1; FPR2;SIGLEC5
	GO:0030659	cytoplasmic vesicle membrane	1.226772047106552E-5	PSENEN;HLADRB5;TYROBP;CR1;SELL;NCF4; FPR1;IRF7;LY96;SIRPB1;SIGLEC5
	GO:0034774	secretory granule lumen	8.887911522711858E-5	PLAC8;SRGN;GCA;GMFG;S100A12;RNASE2; MMP8;S100A9;S100A8
	GO:0035579	specific granule membrane	1.8064502767407338E-4	MMP25;CLEC4D;OLR1;FPR2;GPR84
	GO:0042581	specific granule	3.2742843178608567E-4	MMP25;CLEC4D;OLR1;GPR84;FPR2;MMP8
	GO:0045335	phagocytic vesicle	0.002661302293846886	GNLY;NCF4;RAC2;CLEC4E

(*Continued*)

Table 1. (Continued)

Category	GO ID	GO Pathways	P-values	Genes
GO Cellular Component	GO:0030667	secretory granule membrane	6.097577975166167E-10	MGAM;CR1;FCER1G;FPR1;GPR84;FPR2;SIRPB1;MMP25;CLEC4D;TYROBP;SELL;OLR1;CYSTM1;SIGLEC5
	GO:0070820	tertiary granule	2.7444531601972747E-9	MGAM;CLEC4D;CR1;FCER1G;FPR1;OLR1;CYSTM1;GPR84;FPR2;MMP8;SIGLEC5
	GO:0070821	tertiary granule membrane	9.197680245668367E-9	MGAM;FCER1G;CLEC4D;OLR1;CYSTM1;FPR2;GPR84;SIGLEC5
	GO:0101003	ficolin-1-rich granule membrane	5.8340251207518634E-8	MGAM;CR1;FCER1G;CLEC4D;FPR1;FPR2;SIGLEC5
	GO:0101002	ficolin-1-rich granule	1.1269234942705415E-5	MGAM;CLEC4D;CR1;FCER1G;GMFG;FPR1;FPR2;SIGLEC5
	GO:0030659	cytoplasmic vesicle membrane	1.226772047106552E-5	PSENEN;HLADRB5;TYROBP;CR1;SELL;NCF4;FPR1;IRF7;LY96;SIRPB1;SIGLEC5
	GO:0034774	secretory granule lumen	8.887911522711858E-5	PLAC8;SRGN;GCA;GMFG;S100A12;RNASE2;MMP8;S100A9;S100A8
	GO:0035579	specific granule membrane	1.8064502767407338E-4	MMP25;CLEC4D;OLR1;FPR2;GPR84
	GO:0042581	specific granule	3.2742843178608567E-4	MMP25;CLEC4D;OLR1;GPR84;FPR2;MMP8
	GO:0045335	phagocytic vesicle	0.002661302293846886	GNLY;NCF4;RAC2;CLEC4E

https://doi.org/10.1371/journal.pone.0262737.t001

Candidate drug prediction for targeting hub genes between COVID-19 and IPF

For further investigating the significant role of common hub genes, candidate drugs targeting the 22 upregulated hub genes were predicted (Table 3). A total of 155 candidate drugs were identified with adj.P.value < 0.01 (S3 Table). These drugs were further examined to affect molecular activity of 22 hub genes and their downstream molecules, which are displayed as a list (S4 Table). Among these drugs, 11 were predicted to target more than 10 hub molecules, while 69 drugs targeted less than 3 hub molecules.

Discussion

A strong association between COVID-19 and IPF has been previously reported [4,20,21], and IPF was reported as risk factor for COVID-19 [4]. On the contrary, anti-fibrosis therapies are available for inhibiting severe COVID-19 progression [4]. Moreover, COVID-19 has changed the approach to treat IPF patients, since SARS-CoV-2 infection is reported to impact the prognosis of IPF patients [22]. The relevance between COVID-19 and IPF is supposed to be through the association between up- and downregulated genes. One COVID-19 dataset and five IPF datasets were analyzed, the latter are designed to analyze only the lung samples. These datasets were published from 2011 to 2019, ranging from America to East Asia to ensure that our study is broadly representative. Our finding of aberrant expressed genes from 6 GEO datasets suggested that these DEGs influenced the crosstalk between COVID-19 and IPF. In addition, the present study was designed for the identification of hub genes and the prediction of their potential drug, which may enable novel molecular targets as new COVID-19 strategies with antifibrotic treatment.

Given that common DEGs can drive the development of drugs against COVID-19 and IPF, we concentrated on the DEG-related function after dividing upregulated and downregulated

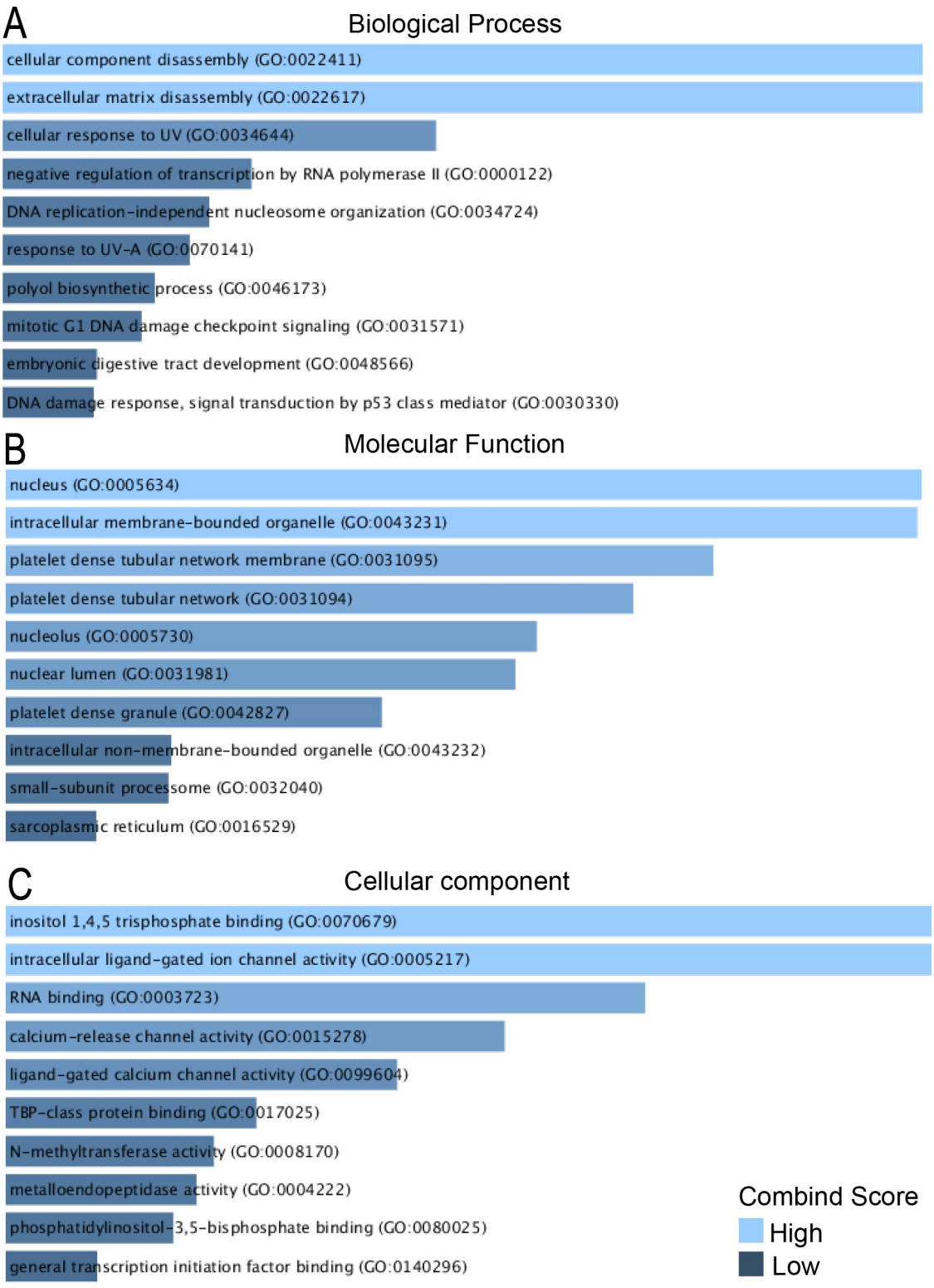

Fig 5. GO terms of downregulated DEGs between COVID-19 and IPF. A: GO analysis of downregulated DEGs according to biological process. B: GO analysis of downregulated DEGs according to molecular function. C: GO analysis of downregulated DEGs according to cellular component.

https://doi.org/10.1371/journal.pone.0262737.g005

Table 2. Go enrichment analysis of downregulated DEGs between COVID-19 and IPF.

Category	GO ID	GO Pathways	P-values	Genes
GO biological process	GO:0022411 GO:0022617 GO:0034644	cellular component disassembly extracellular matrix disassembly cellular response to UV	3.6908055963859072E-6 3.6908055963859072E-6 1.6226306755965077E-4	MMP14;MMP1;SH3PXD2B;A2M; MMP10 MMP14;MMP1;SH3PXD2B;A2M; MMP10 MMP1;XPC;CRIP1;TAF1
	GO:0000122	negative regulation of transcription by RNA polymerase II	6.80695281487198E-4	ZNF451;CCND1;GADD45A;ATRX; CTR9; TCF21;NR1D2;TBX2;TAF1
	GO:0034724	DNA replication-independent nucleosome organization	9.449631056544972E-4	NASP;ATRX
	GO:0070141	response to UV-A	0.0010999291367171904	CCND1;MMP1
	GO:0046173	polyol biosynthetic process	0.001443814289271468	ITPKB;ISYNA1
	GO:0031571	mitotic G1 DNA damage checkpoint signaling	0.001599460082312502	CCND1;PRMT1;GADD45A
	GO:0048566	embryonic digestive tract development	0.002265165629135075	RARRES2;TCF21
	GO:0030330	DNA damage response, signal transduction by p53 class mediator	0.0023202515386528087	PRMT1;GADD45A;ATRX
GO Molecular Function	GO:0070679	inositol 1,4,5 trisphosphate binding	6.693872237504711E-4	ITPR1;ITPR3
	GO:0005217	intracellular ligand-gated ion channel activity	6.693872237504711E-4	ITPR1;ITPR3
	GO:0003723	RNA binding	0.0012169581083683082	PTCD3;UTP6;PRMT1;RNMT;DDX42; CIRBP; URB1;GNL2;MFAP1;MPHOSPH10; TSR1;PPIG; SREK1
	GO:0015278	calcium-release channel activity	0.001632573414944103	ITPR1;ITPR3
	GO:0099604	ligand-gated calcium channel activity	0.0020433278549486355	ITPR1;ITPR3
	GO:0017025	TBP-class protein binding	0.002741371475892866	PSMC5;TAF1
	GO:0008170	N-methyltransferase activity	0.0029955844322773523	PRMT1;RNMT
	GO:0004222	metalloendopeptidase activity	0.003106381363248335	MMP14;MMP1;MMP10
	GO:0080025	phosphatidylinositol-3,5-bisphosphate binding	0.003260434667143527	SH3PXD2B;WIPI1
	GO:0140296	general transcription initiation factor binding	0.003821741127686192	PSMC5;TAF1
GO Cellular Component	GO:0005634	nucleus	0.000147678458404248	ZNF451;ATF6B;RNMT;DDX42;TCF21; DLST; STC1;XPC;TRAK1;CCND1;HMOX1; RALGDS;EGR1;PRMT1;GADD45A; ZNF160; ATRX;CIRBP;NR1D2;GNL2;TBX2; ITPKB; GCHFR;MMP14;PSMC5;NASP;MFAP1; HBP1; PPIG;TAF1
	GO:0043231	intracellular membrane-bounded organelle	0.000151288413440493	ZNF451;ATF6B;RNMT;DDX42;ITPR1; TCF21; DLST;STC1;XPC;TRAK1;CCND1; PODXL; HMOX1;RALGDS;EGR1;PRMT1; GADD45A; ZNF160;ATRX;CIRBP;NR1D2;GNL2; TBX2; ITPKB;GCHFR;MMP14;PSMC5;NASP; MFAP1; RAPGEF1;HBP1;PPIG;TAF1
	GO:0031095	platelet dense tubular network membrane	0.000440161889353639	ITPR1;ITPR3
	GO:0031094	platelet dense tubular network	0.000669387223750471	ITPR1;ITPR3

(*Continued*)

Table 2. (Continued)

Category	GO ID	GO Pathways	P-values	Genes
	GO:0005730	nucleolus	0.00110914228877878	SELENBP1;UTP6;PODXL;MPHOSPH10; TSR1; XPC;URB1;GNL2;TAF1
	GO:0031981	nuclear lumen	0.00124200795340088	SELENBP1;UTP6;PODXL;MPHOSPH10; TSR1; XPC;URB1;GNL2;TAF1
	GO:0042827	platelet dense granule	0.00249787275567805	RARRES2;ITPR1
	GO:0043232	intracellular non-membrane-bounded organelle	0.00752249102119212	SELENBP1;UTP6;PODXL;SH3PXD2B; MPHOSPH10;TSR1;XPC;URB1;GNL2; TAF1
	GO:0032040	small-subunit processome	0.0076371805235121	UTP6;MPHOSPH10
	GO:0016529	sarcoplasmic reticulum	0.0111473609254622	ITPR1;ITPR3

https://doi.org/10.1371/journal.pone.0262737.t002

genes. Except for immune response and defense response to virus, it is somewhat surprising that upregulated DEGs are enriched in inflammatory molecules, especially cytokine-related function. Type I interferon signaling pathway and cytokine-mediated signaling pathway were mainly related to upregulated DEGs. An association between type I interferon and IPF has been reported to show that type I interferon pathway may drive chronic inflammation and fibrosis [23]. Type I interferon response was amplified based on ex vivo evidence of IPF [24]. It has been reported that there were similar cytokine profiles in IPF and COVID-19 [22], which is consistent with an observation that the level of profibrotic mediators in COVID-19 patients was increased at the serum level. Our finding was an important evidence to support an antifibrotic therapy for COVID-19 patients by mediating cytokine signaling.

In case of downregulated genes between COVID-19 and IPF, the biological function was enriched in disassembly of cellular components and extracellular matrix. The pathological changes in IPF developed from an alteration of extracellular matrix, which can replace the healthy lung tissue, contributing to the deterioration of lung compliance [25]. The lung architecture is destructed due to the secretion of excessive amounts of extracellular matrix from fibroblast and myofibroblast foci [26]. Our findings were in accordance with the previous research. In our study, matrix metalloproteinases (MMPs) which accounted for disassembly of extracellular matrix were downregulated in both COVID-19 and IPF. These findings may help us to understand that absence of these genes in COVID-19 patients might induce the progression to fibrosis.

The common hub genes between COVID-19 and IPF were the most strongly associated among all DEGs. The hub genes were indeed relevant with IPF progression. For example, our study revealed that several hub genes were related to interferon signal pathway, which was demonstrated to influence IPF treatment. Besides, 19 hub genes are involved in the enrichment of chemokines. Previous research showed that chemokine CCL2 and its downstream pathways were the key to the development of IPF [27]. Our findings from PPI network analysis were consistent with our above functional enrichment, suggesting that these hub genes could be novel therapeutic targets between COVID-19 and IPF.

Considering that the hub genes played a vital role in a crosstalk between COVID-19 and IPF, we used hub genes to identify potential candidate drugs. We found several potential candidate drugs which probably contributed to the treatment of COVID-19 and IPF. Among all candidate drugs, the current study highlights the top 10 significant drugs. Among them, candidate drugs targeting exogenous invasion enabled to be an important approach along with suloctidil, which has been suggested as potential antifungal agent [28]. 3'-Azido-3'-deoxythymidine CTD 00007047 was used as an anti-viral agent and a reverse transcriptase inhibitor

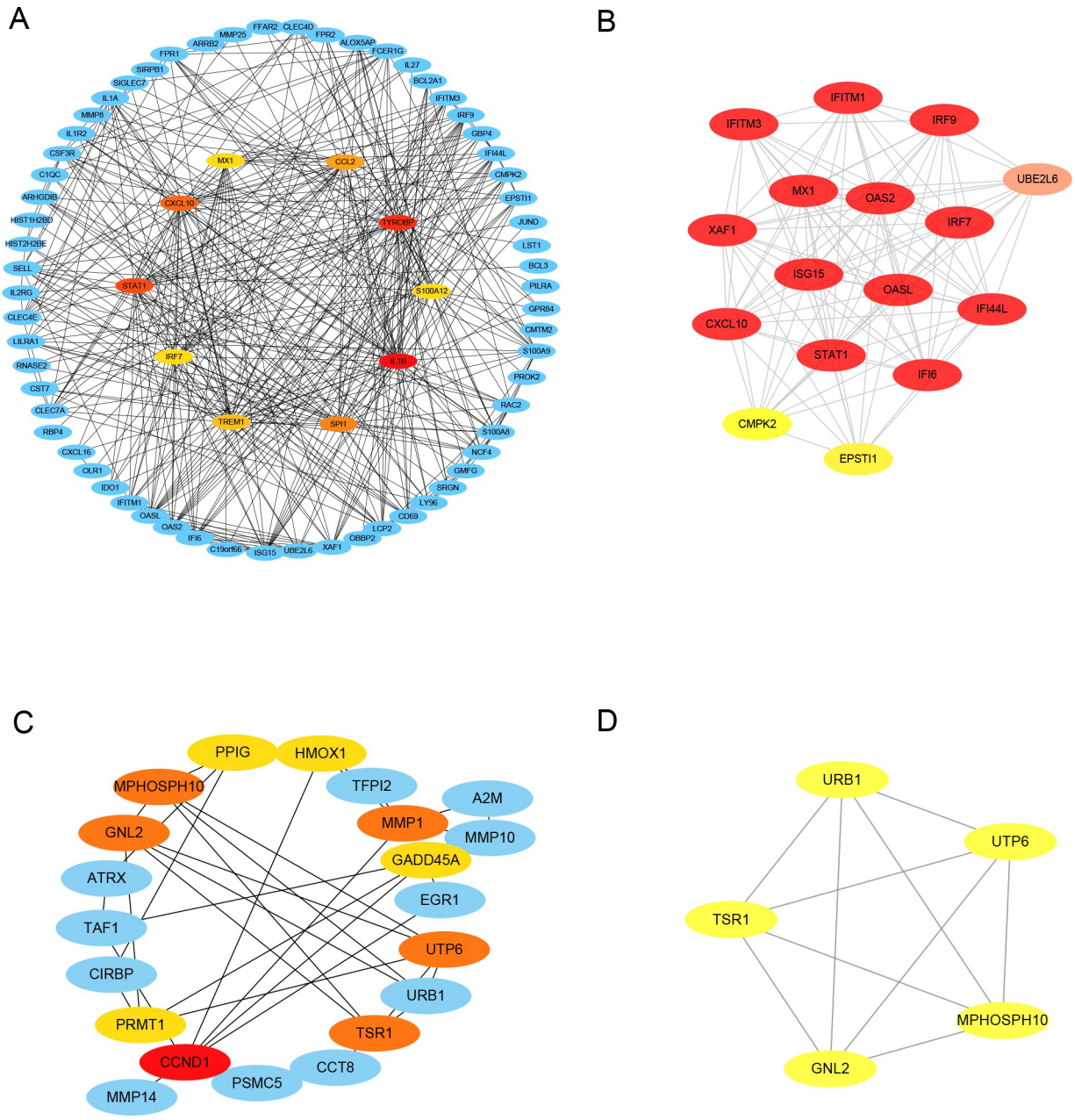

Fig 6. Identification of hub genes from PPI network using Cytoscape plugins Cytohubba and MCODE. A: Hub genes identified among upregulated genes using Cytohubba plugin in Cytoscape software. B: Hub genes identified among upregulated genes using MCODE plugin in Cytoscape software. C: Hub genes identified among downregulated genes using Cytohubba plugin in Cytoscape software. D: Hub genes identified among downregulated genes using MCODE plugin in Cytoscape software.

https://doi.org/10.1371/journal.pone.0262737.g006

active against HIV-1, and thioridazine was proved to exhibit anti-viral activity [29]. Moreover, a previous study has revealed that myofibroblast activation and uncontrolled proliferation associated IPF with cancer [30]. Several candidate drugs exhibit anticancer activities. Chlorophyllin CTD 00000324 was determined to deactivate ERKs and inhibit breast cancer cell proliferation [31]. Prochlorperazine has been proved to exhibit anticancer activity towards different types of human cancer [32]. Terfenadine, demonstrated to be effective against PC-3 and DU-145 cells (two prostate cancer cell lines) by inducing cell apoptosis [33], and etoposide were

Table 3. Prediction of TOP 10 candidate drugs for high expressed hub genes.

Name of drugs	P-value	Adjusted P-value	Genes
suloctidil HL60 UP	1.17603903224093E-25	1.27835442804589E-22	IFITM1;STAT1;MX1;IFI6;UBE2L6;ISG15; IFI44L;OASL;CXCL10;OAS2;IRF7; CCL2;XAF1;IRF9
prenylamine HL60 UP	1.06795174564932E-22	5.80431773760409E-20	CXCL10;STAT1;MX1;IFI6;IRF7; ISG15;XAF1;IFI44L;IRF9;OASL
acetohexamide PC3 UP	2.44772613152278E-19	8.86892768321756E-17	IFITM1;STAT1;OAS2;MX1;IFI6; IFI44L;IRF9;OASL
chlorophyllin CTD 00000324	1.34723424808812E-15	3.66110906917947E-13	CXCL10;IFITM1;STAT1;OAS2; MX1;IFI6;ISG15
3'-Azido-3'-deoxythymidine CTD 00007047	4.95534561362891E-14	1.07729213640292E-11	IFITM1;STAT1;OAS2;IL1B;MX1; IFI6;IRF7;EPSTI1;CCL2;ISG15;IFI44L
prochlorperazine MCF7 UP	1.95377160519666E-13	3.53958289141462E-11	IFITM1;STAT1;IFI6;IRF7;ISG15; IRF9;OASL
terfenadine HL60 UP	2.50627914129244E-13	3.89189346654984E-11	STAT1;MX1;IFI6;IRF7;ISG15; XAF1;IRF9
etoposide HL60 UP	2.05940731534332E-12	2.79821968972273E-10	STAT1;IL1B;MX1;IFI6;IRF7; CCL2;ISG15;IRF9
Arsenenous acid CTD 00000922	8.47115116155285E-11	1.02312681251199E-08	IFITM3;IFITM1;STAT1;MX1; IFI6;UBE2L6;ISG15;IFI44L;CXCL10; OAS2;IL1B;CCL2;XAF1
propofol MCF7 UP	3.01735334589948E-09	3.27986308699273E-07	IFITM1;IFI6;ISG15;IRF9;OASL

https://doi.org/10.1371/journal.pone.0262737.t003

identified as anticancer drugs as they induced cancer cell apoptosis [34]. It can be assumed that candidate drugs which possess anticancer activity with the inhibition of cell proliferation and fibroblast activation might contribute to the treatment of IPF and COVID-19. In summary, the present study raised the possibility that existing drug and compounds may be available for the development of COVID-19 therapy.

Although the risk factors for IPF and COVID-19 are common, our study provides insufficient evidence to support the clinical practice of candidate drug for COVID-19 and IPF treatment. Furthermore, due to this limitation, the downstream molecules of hub genes should be determined in the future, and the role of the hub genes in crosstalk between COVID-19 and IPF should be confirmed using clinical samples and experimental models. Although the current research against COVID-19 has been conducted and data on COVID-19 in GEO are rapidly enriched, GSE147507 dataset has been verified to be reliable with solid evidence. Our conclusions were based on the responses of 5 GSEs in GEO database and so might not reflect processes via the in vivo and in vitro experiments.

Conclusion

In summary, our results provide the common DEGs between COVID-19 and IPF, which add to the accumulating evidence that suggests a treatment for COVID-19 patients in the pulmonology ward administered antifibrotic therapy. With a series of enrichment analysis, herein, we offer new insights into the development of COVID-19 treatment on the basis of biological function. The current study unveiled a potential role of hub genes in COVID-19 and IPF, contributing to a combined COVID-19 treatment. Moreover, our findings offer some suggestions on therapeutic target identification in diseases caused by the Delta SARS-CoV-2 variant, when the common risk factor of the Delta associated with a distinct disease will be uncovered.

Supporting information

S1 Fig. Pathway-based enrichment analysis of upregulated DEGs between COVID-19 and IPF. Biological entity of upregulated DEGs between COVID-19 and IPF in Wikipathways (A), KEGG (B), Reactome (C), and Biocarta (D).
(TIF)

S2 Fig. Pathway-based enrichment analysis of downregulated DEGs between COVID-19 and IPF. Biological entity of downregulated DEGs between COVID-19 and IPF in Wikipathways (A), KEGG (B), Reactome (C), and Biocarta (D).
(TIF)

S3 Fig. GO and KEGG functional enrichment analysis of upregulated hub genes. GO analysis of upregulated hub genes according to biological process (A), molecular function (B) and cellular component (C). The results of pathway terms through KEGG analysis of upregulated hub genes(D).
(TIF)

S4 Fig. GO and KEGG functional enrichment analysis of downregulated hub genes. GO analysis of downregulated hub genes according to biological process (A), molecular function (B) and cellular component (C). The results of pathway terms through KEGG analysis of downregulated hub genes(D).
(TIF)

S1 Table. Pathway enrichment analysis of upregulated DEGs between COVID-19 and IPF.
(DOCX)

S2 Table. Pathway enrichment analysis of downregulated DEGs between COVID-19 and IPF.
(DOCX)

S3 Table. Prediction of candidate drugs for upregulated hub genes.
(DOCX)

S4 Table. The downstream molecules of 22 hub genes.
(DOCX)

Acknowledgments

The authors sincerely acknowledge the Helixlife (www.xiantao.love) for some bioinformatics approaches to explore the databases.

Author Contributions

Conceptualization: Shilin Xia.

Data curation: Qianyi Chen.

Formal analysis: Qianyi Chen.

Investigation: Xueying Shi, Bingqian Huang.

Methodology: Qianyi Chen.

Project administration: Shilin Xia.

Resources: Xueying Shi, Bingqian Huang.

Software: Tingxin Wang.

Supervision: Hua Sui.

Validation: Hua Sui.

Visualization: Qianyi Chen.

Writing – original draft: Qianyi Chen.

Writing – review & editing: Qianyi Chen, Shilin Xia.

References

1. Lu R, Zhao X, Li J, Niu P, Yang B, Wu H, et al. Genomic characterisation and epidemiology of 2019 novel coronavirus: implications for virus origins and receptor binding. Lancet. 2020; 395(10224):565–74. https://doi.org/10.1016/S0140-6736(20)30251-8 PMID: 32007145
2. Jiang F, Deng L, Zhang L, Cai Y, Cheung CW, Xia Z. Review of the Clinical Characteristics of Coronavirus Disease 2019 (COVID-19). J Gen Intern Med. 2020; 35(5):1545–9. https://doi.org/10.1007/s11606-020-05762-w PMID: 32133578
3. George PM, Patterson CM, Reed AK, Thillai M. Lung transplantation for idiopathic pulmonary fibrosis. Lancet Respir Med. 2019; 7(3):271–82. https://doi.org/10.1016/S2213-2600(18)30502-2 PMID: 30738856
4. George PM, Wells AU, Jenkins RG. Pulmonary fibrosis and COVID-19: the potential role for antifibrotic therapy. Lancet Respir Med. 2020; 8(8):807–15. https://doi.org/10.1016/S2213-2600(20)30225-3 PMID: 32422178
5. Edgar R, Domrachev M, Lash AE. Gene Expression Omnibus: NCBI gene expression and hybridization array data repository. Nucleic Acids Res. 2002; 30(1):207–10. https://doi.org/10.1093/nar/30.1.207 PMID: 11752295
6. Barrett T, Wilhite SE, Ledoux P, Evangelista C, Kim IF, Tomashevsky M, et al. NCBI GEO: archive for functional genomics data sets—update. Nucleic Acids Res. 2013; 41(Database issue):D991–5. https://doi.org/10.1093/nar/gks1193 PMID: 23193258
7. Blanco-Melo D, Nilsson-Payant BE, Liu WC, Uhl S, Hoagland D, Moller R, et al. Imbalanced Host Response to SARS-CoV-2 Drives Development of COVID-19. Cell. 2020; 181(5):1036–45 e9. https://doi.org/10.1016/j.cell.2020.04.026 PMID: 32416070
8. Daamen AR, Bachali P, Owen KA, Kingsmore KM, Hubbard EL, Labonte AC, et al. Comprehensive transcriptomic analysis of COVID-19 blood, lung, and airway. Sci Rep. 2021; 11(1):7052. https://doi.org/10.1038/s41598-021-86002-x PMID: 33782412
9. Negreros M, Hagood JS, Espinoza CR, Balderas-Martinez YI, Selman M, Pardo A. Transforming growth factor beta 1 induces methylation changes in lung fibroblasts. PLoS One. 2019; 14(10): e0223512. https://doi.org/10.1371/journal.pone.0223512 PMID: 31603936
10. Cecchini MJ, Hosein K, Howlett CJ, Joseph M, Mura M. Comprehensive gene expression profiling identifies distinct and overlapping transcriptional profiles in non-specific interstitial pneumonia and idiopathic pulmonary fibrosis. Respir Res. 2018; 19(1):153. https://doi.org/10.1186/s12931-018-0857-1 PMID: 30111332
11. Horimasu Y, Ishikawa N, Taniwaki M, Yamaguchi K, Hamai K, Iwamoto H, et al. Gene expression profiling of idiopathic interstitial pneumonias (IIPs): identification of potential diagnostic markers and therapeutic targets. BMC Med Genet. 2017; 18(1):88. https://doi.org/10.1186/s12881-017-0449-9 PMID: 28821283
12. DePianto DJ, Chandriani S, Abbas AR, Jia G, N'Diaye EN, Caplazi P, et al. Heterogeneous gene expression signatures correspond to distinct lung pathologies and biomarkers of disease severity in idiopathic pulmonary fibrosis. Thorax. 2015; 70(1):48–56. https://doi.org/10.1136/thoraxjnl-2013-204596 PMID: 25217476
13. Meltzer EB, Barry WT, D'Amico TA, Davis RD, Lin SS, Onaitis MW, et al. Bayesian probit regression model for the diagnosis of pulmonary fibrosis: proof-of-principle. BMC Med Genomics. 2011; 4:70. https://doi.org/10.1186/1755-8794-4-70 PMID: 21974901
14. Shpiner R, Vathi S, Stuckey DC. Treatment of oil well "produced water" by waste stabilization ponds: removal of heavy metals. Water Res. 2009; 43(17):4258–68. https://doi.org/10.1016/j.watres.2009.06.004 PMID: 19580985
15. Kanehisa M, Goto S. KEGG: kyoto encyclopedia of genes and genomes. Nucleic Acids Res. 2000; 28 (1):27–30. https://doi.org/10.1093/nar/28.1.27 PMID: 10592173

16. Slenter DN, Kutmon M, Hanspers K, Riutta A, Windsor J, Nunes N, et al. WikiPathways: a multifaceted pathway database bridging metabolomics to other omics research. Nucleic Acids Res. 2018; 46(D1): D661–D7. https://doi.org/10.1093/nar/gkx1064 PMID: 29136241

17. Fabregat A, Jupe S, Matthews L, Sidiropoulos K, Gillespie M, Garapati P, et al. The Reactome Pathway Knowledgebase. Nucleic Acids Res. 2018; 46(D1):D649–D55. https://doi.org/10.1093/nar/gkx1132 PMID: 29145629

18. Szklarczyk D, Gable AL, Nastou KC, Lyon D, Kirsch R, Pyysalo S, et al. The STRING database in 2021: customizable protein-protein networks, and functional characterization of user-uploaded gene/measurement sets. Nucleic Acids Res. 2021; 49(D1):D605–D12. https://doi.org/10.1093/nar/gkaa1074 PMID: 33237311

19. Yoo M, Shin J, Kim J, Ryall KA, Lee K, Lee S, et al. DSigDB: drug signatures database for gene set analysis. Bioinformatics. 2015; 31(18):3069–71. https://doi.org/10.1093/bioinformatics/btv313 PMID: 25990557

20. Zhang C, Wu Z, Li JW, Tan K, Yang W, Zhao H, et al. Discharge may not be the end of treatment: Pay attention to pulmonary fibrosis caused by severe COVID-19. J Med Virol. 2021; 93(3):1378–86. https://doi.org/10.1002/jmv.26634 PMID: 33107641

21. Uzel FI, Iliaz S, Karatas F, Caglayan B. COVID-19 Pneumonia and Idiopathic Pulmonary Fibrosis: A Novel Combination. Turk Thorac J. 2020; 21(6):451–3. https://doi.org/10.5152/TurkThoracJ.2020.20123 PMID: 33352102

22. Mishra M, Sindhwani G. Antifibrotics for COVID-19 related lung fibrosis: Agents with benefits? Adv Respir Med. 2021; 89(2):231–3. https://doi.org/10.5603/ARM.a2021.0023 PMID: 33966265

23. Vigeland CL, Hughes AH, Horton MR. Etiology and treatment of cough in idiopathic pulmonary fibrosis. Respir Med. 2017; 123:98–104. https://doi.org/10.1016/j.rmed.2016.12.016 PMID: 28137504

24. Fraser E, Denney L, Antanaviciute A, Blirando K, Vuppusetty C, Zheng Y, et al. Multi-Modal Characterization of Monocytes in Idiopathic Pulmonary Fibrosis Reveals a Primed Type I Interferon Immune Phenotype. Front Immunol. 2021; 12:623430. https://doi.org/10.3389/fimmu.2021.623430 PMID: 33746960

25. Richeldi L, Collard HR, Jones MG. Idiopathic pulmonary fibrosis. Lancet. 2017; 389(10082):1941–52. https://doi.org/10.1016/S0140-6736(17)30866-8 PMID: 28365056

26. King TE Jr., Pardo A, Selman M. Idiopathic pulmonary fibrosis. Lancet. 2011; 378(9807):1949–61. https://doi.org/10.1016/S0140-6736(11)60052-4 PMID: 21719092

27. Brody SL, Gunsten SP, Luehmann HP, Sultan DH, Hoelscher M, Heo GS, et al. Chemokine Receptor 2-targeted Molecular Imaging in Pulmonary Fibrosis. A Clinical Trial. Am J Respir Crit Care Med. 2021; 203(1):78–89. https://doi.org/10.1164/rccm.202004-1132OC PMID: 32673071

28. Zeng B, Li J, Wang Y, Chen P, Wang X, Cui J, et al. In vitro and in vivo effects of suloctidil on growth and biofilm formation of the opportunistic fungus Candida albicans. Oncotarget. 2017; 8(41):69972–82. https://doi.org/10.18632/oncotarget.19542 PMID: 29050256

29. Thanacoody HK. Thioridazine: resurrection as an antimicrobial agent? Br J Clin Pharmacol. 2007; 64 (5):566–74. https://doi.org/10.1111/j.1365-2125.2007.03021.x PMID: 17764469

30. Ballester B, Milara J, Cortijo J. Idiopathic Pulmonary Fibrosis and Lung Cancer: Mechanisms and Molecular Targets. Int J Mol Sci. 2019; 20(3). https://doi.org/10.3390/ijms20030593 PMID: 30704051

31. Chiu LC, Kong CK, Ooi VE. The chlorophyllin-induced cell cycle arrest and apoptosis in human breast cancer MCF-7 cells is associated with ERK deactivation and Cyclin D1 depletion. Int J Mol Med. 2005; 16(4):735–40. PMID: 16142413

32. Otreba M, Kosmider L. In vitro anticancer activity of fluphenazine, perphenazine and prochlorperazine. A review. J Appl Toxicol. 2021; 41(1):82–94. https://doi.org/10.1002/jat.4046 PMID: 32852120

33. Wang WT, Chen YH, Hsu JL, Leu WJ, Yu CC, Chan SH, et al. Terfenadine induces anti-proliferative and apoptotic activities in human hormone-refractory prostate cancer through histamine receptor-independent Mcl-1 cleavage and Bak up-regulation. Naunyn Schmiedebergs Arch Pharmacol. 2014; 387 (1):33–45. https://doi.org/10.1007/s00210-013-0912-x PMID: 24048439

34. Genin M, Clement F, Fattaccioli A, Raes M, Michiels C. M1 and M2 macrophages derived from THP-1 cells differentially modulate the response of cancer cells to etoposide. BMC Cancer. 2015; 15:577. https://doi.org/10.1186/s12885-015-1546-9 PMID: 26253167